Chemical Engineering Journal 154 (2009) 120–130

Contents lists available at ScienceDirect

Chemical Engineering Journal

journal homepage: www.elsevier.com/locate/cej

Comparison of external mass transfer approaches for heterogeneously catalyzed hydrogenation of vaporized hydrocarbons

A.B. Shigarov*, V.A. Kirillov

Boreskov Institute of Catalysis (BIC), pr. Lavrentyeva 5, 630090, Novosibirsk, Russia

ARTICLE INFO

Article history:
Received 12 December 2008
Received in revised form 1 April 2009
Accepted 6 April 2009

Keywords:
Gas-phase hydrogenation of hydrocarbons
Multicomponent diffusion
External mass and heat transfer
Maxwell–Stefan equations
Film model

ABSTRACT

The catalytic hydrogenation of vaporized α-methylstyrene (AMS) and 1-octene under external transfer control is tested by different interphase mass transfer approaches. The previously reported experimental data on temperature measurements in the single-pellet reactor and the new experimental data in a fixed-bed reactor are analyzed theoretically. The independent diffusion (Fick) approach absolutely failed to fit the experiments. Three methods that take into account multicomponent diffusion (and are based on the Maxwell–Stefan equations) give close results and agree well with the experimental data. Nevertheless, for hydrogenation (or dehydrogenation) of vaporized hydrocarbons the pseudo-binary approach considered in this study is recommended. It is very simple to use even in a case of complex mixture of hydrocarbons and/or several hydrogenation reactions, when general approaches demanded cumbersome matrix operations. Another more fundamental advantage of the pseudo-binary treatment is that the usage of traditional empirical correlations $Sh(Re, Sc)$, $Nu(Re, Pr)$ for gas–solid transfer (which, as a rule, are based on the Chilton–Colburn analogy) gets the solid theoretical background.

1. Introduction

Many of chemical processes involve heterogeneous hydrogenation of hydrocarbons in a fixed catalytic bed. Hydrogenation reactions are characterized by high heat effects and fast intrinsic kinetics that results in an important impact of the external transfer, especially if hydrocarbons are vaporized [1–3], as in the gas-phase reactors with a bundle of externally cooled tubes or in trickle-bed reactors with a volatile liquid phase.

The first question that arises here is what diffusion theory should be used: independent (Fick) or multicomponent. In a strict sense, the usage of independent diffusion (Fick) approach is valid only for the following two cases [4,5]:

1. All binary diffusion coefficients are nearly equal, $D_{ij} \approx D = \text{const}$ (e.g. binary mixture).
2. The mixture is dilute, having a sufficiently low content of the transferred component.

Both cases correspond to the experimental conditions at which most empirical mass transfer correlations have been obtained. The Chilton–Colburn analogy for the heat and mass transfer also holds only for these cases. In the gas-phase (de)hydrogenation of hydrocarbons, physical properties (e.g. binary diffusion coefficients) of hydrogen and two other heavy components may differ by more than one order of magnitude. Moreover, despite small molar fractions of heavy reagent (hydrocarbon) in a mixture with light reagent (hydrogen), the diffusion friction among a pair of hydrocarbons (reagent and product) can be very significant. Consequently, multicomponent diffusion approach based on the Maxwell–Stefan equations should be employed [5,6].

Furthermore, an important issue is the estimation of the average (effective) film thickness related to the external mass transfer. Conventional empirical correlations (at forced convection) define this thickness as $h_D = d/Sh(Re, Sc)$, $Sc = \nu/D$, where single coefficient D reflects the physical property of the mixture. But the Maxwell–Stefan equations include a set of binary coefficients D_{ij}. One of the first solutions of this hurdle was given by the linearized theory of multicomponent diffusion [7,8]. The application of this theory requires difficult and time-consuming matrix algebra operations and so far is rarely used for reactor modeling, e.g. [2]. Essentially simplified approach based directly on the Maxwell–Stefan equations was suggested in [6,10] and recommended for engineering purposes.

Other simplified multicomponent approaches that are based on application of an effective diffusion concept are considered in [5]. For heterogeneously catalyzed reactions, the effective diffusion coefficients (called sometimes pseudo-binary) inevitably depend on the reaction stoichiometry and consequently have no physical sense. Strictly speaking, such “diffusion coefficients” are incompat-

---

* Corresponding author.
E-mail address: shigarov@catalysis.nsk.su (A.B. Shigarov).

1385-8947/$ – see front matter © 2009 Elsevier B.V. All rights reserved.
doi:10.1016/j.cej.2009.04.015

Nomenclature

A_F	Ackermann correction factor
$a = \lambda/(C_b \rho)$	coefficient of gas mixture thermal conductivity (m^2/s)
C_b	specific molar heat capacity of a gas mixture (J/(mol K))
D_0	pseudo-binary diffusion coefficient (m^2/s)
D_{ij}	binary diffusion coefficient (i, j = A, B, H) (m^2/s)
d	pellet diameter (m)
$h_d = d/Sh$	diffusion film effective thickness (m)
$h_h = d/Nu$	thermal film effective thickness (m)
$\vec{J}, \vec{J'}$	vector of ordinary and linearly transformed molar fluxes (via diffusion) (mol/(m^2 s))
J_i	molar flux (via diffusion) of gas components (i = A, B, H) (mol/(m^2 s))
K_R	equilibrium constant for reversible reaction (N/m^2)
L	length of the fixed-bed reactor (m)
ℓ	coordinate across the external diffusion film (m)
m_i	molecular mass of gas components (i = A, B, H) (kg/mol)
N_i	total flux of gas component (i = A, B, H) across the external diffusion film (mol/(m^2 s))
N_{tot}	total flux of gas mixture across the external diffusion film (mol/(m^2 s))
N	molar flux of gas mixture in the axial direction of a fixed-bed reactor (mol/(m^2 s))
n	stoichiometric coefficient
P	pressure (N/m^2)
Q	heat of reaction (J/mol)
R	ideal gas constant (8.31 J/(mol K))
r	volumetric apparent reaction rate in a fixed-bed reactor (mol/(m^3(bed) s))
S	specific geometric surface of a bed (m^{-1})
T	temperature (K or C)
$[T]$	matrix, composed by eigenvectors
$\vec{t}_1, \vec{t}_2$	eigenvectors
u	gas linear velocity in a fixed-bed reactor (m/s)
W	pellet surface apparent reaction rate (mol/(m^2 s))
$\vec{\mathbf{x}}, \vec{\mathbf{x}}'$	vector of ordinary and linearly transformed mole fractions
X_{AMS}	AMS conversion
x	mole fraction of transport-limiting component
x_i	mole fraction of a component (i = A, B, H) in gas mixture
$\tilde{x}_i$	reference mole fraction of component (i = A, B, H) inside the film
$y_{Ab} = (x_{Ab}/(x_{Ab} + x_{Bb}))$	mole fraction of A in vapor mixture of A and B (after excluding H_2)
z	axial coordinate in a fixed-bed reactor (m)
z'	dimensionless axial coordinate in a fixed-bed reactor

Dimensionless groups

$Le = a/D_0$	Lewis number
Nu	Nusselt number
$Pr = \nu/a$	Prandtl number
Re	Reynolds number
$Sc = \nu/D$	Schmidt number
Sh	Sherwood number

Greek letters

α	heat transfer coefficient (W/(m^2 K))
β	mass transfer coefficient for limiting component in binary or diluted mixture (m/s)
β_{ij}	binary mass transfer coefficients for gas mixture components (i, j = A, B, H) (m/s)
λ	heat conductivity coefficient of gas mixture (W/(m K))
λ_i	heat conductivity coefficient of gas mixture components (i = A, B, H) (W/(m K))
ν	kinematic viscosity of gas mixture (m^2/s)
$\rho = P/RT_b$	molar density of gas mixture (mol/m^3)
ϕ	heat transfer rate factor
$\Delta T = (T_s - T_b)$	bulk (gas)-catalyst pellet temperature rise (difference)
ΔT_{ad}	adiabatic temperature rise

Subscripts and superscripts

A	heavy reagent (hydrocarbon: AMS or 1-octene)
B	heavy product (hydrocarbon: cumene or *n*-octane)
b	bulk (gas flow)
eq	equivalent
exp	experimental value
H	light reagent (hydrogen)
in	inlet
out	outlet
s	catalyst pellet surface

ible with conventional interphase mass transfer correlations based on Chilton–Colburn analogy.

From time to time, different researchers continue to suggest simplified approaches to multicomponent mass transfer, see e.g. [11,12], by taking into account a specificity of a particular problem. Our earlier paper [13] has suggested the original pseudo-binary treatment of multicomponent mass transfer for a gas-phase hydrogenation of heavy hydrocarbons, and this approach was successfully tested by the temperature measurements during benzene vapor hydrogenation on a single catalyst pellet Pt/Al_2O_3. The same approach was successfully applied to modeling of critical phenomena (ignition, extinction, hysteresis) for α-methylstyrene (AMS) hydrogenation on a partially wetted catalyst pellet [3]. However, the suggested approach was not yet confirmed by theoretical background.

The aim of this paper is to provide a more rigorous theoretical consideration of the pseudo-binary approach within a film model and to compare it with general multicomponent approaches. All theoretical approaches are tested with the previously reported in [1] experimental data on temperature measurements in the single-pellet reactor for AMS and 1-octene hydrogenation and the new experimental data in a fixed-bed reactor (AMS vapor hydrogenation) under external transfer control.

2. Experimental

The following reactions were used:

- hydrogenation of AMS to cumene: $C_9H_{10} + H_2 = C_9H_{12}$;
- hydrogenation of 1-octene to *n*-octane: $C_8H_{16} + H_2 = C_8H_{18}$.

2.1. Single-pellet reactor experiments

The details of the experimental setup and procedures are given in [1]. A catalyst pellet (5 mm height and diameter cylinder 3.5% $Pd/\gamma Al_2O_3$ or 15% $Pt/\gamma Al_2O_3$) was fixed on a sufficiently rigid thermocouple that was inserted at the pellet center through the finely drilled channel. This original installation enables to measure the solid temperature accurately without the influence of the thermal boundary layer. The temperature of the gas flow (hydrocarbon vapor and hydrogen) was measured by the second thermocouple that was placed at 3 mm up-flow from the pellet surface. The temperature difference between the gas bulk and the pellet (so-called "gas-pellet temperature rise") was measured as a function of the Reynolds number, gas flow temperature and vapor fraction in a mixture with hydrogen.

2.2. Fixed-bed reactor experiments

The setup included a quartz tube reactor with internal diameter 9.5 mm, a system for supplying liquid AMS and hydrogen into reactor, a liquid AMS vaporizer, a vapor-hydrogen mixer, a condenser of vapors at the outlet, a chromatographic system for analyzing the concentrations of AMS and cumene in the condensed liquid. The reactor was packed with catalyst 3.5% Pd/γAl_2O_3 (spherical particles with the average diameter 2–3 mm) with two different catalyst bed heights 12 and 20 mm. Hydrogen was fed with a constant flow rate 25 cm^3/s; liquid AMS was fed into vaporizer with three different flow rates 32, 45 and 64 mg/s. Hydrogen mixed with the AMS vapor was heated to the inlet temperature 140 °C (which was kept constant) and fed to the reactor inlet. At the reactor outlet the vaporized mixture of AMS and produced cumene was condensed and analyzed chromatographically, and by this way the AMS conversion was determined (52–71%).

3. Theory

In this study we consider the reaction of the gas-phase hydrocarbon hydrogenation ($n > 0$) or dehydrogenation ($n < 0$) according to scheme:

$$A + nH_2 = B, \tag{1}$$

where A is a (de)hydrogenated hydrocarbon, B is a reaction product, and n is the stoichiometric coefficient for hydrogen. The one-dimensional Maxwell–Stefan equations [4,5] for a ternary ideal gas mixture (A, B, H_2) take the form:

$$\rho\frac{dx_A}{d\ell} = \frac{x_AN_H - x_HN_A}{D_{AH}} + \frac{x_AN_B - x_BN_A}{D_{AB}} = \frac{x_AJ_H - x_HJ_A}{D_{AH}} + \frac{x_AJ_B - x_BJ_A}{D_{AB}}, \tag{2}$$

$$\rho\frac{dx_B}{d\ell} = \frac{x_BN_H - x_HN_B}{D_{BH}} + \frac{x_BN_A - x_AN_B}{D_{AB}} = \frac{x_BJ_H - x_HJ_B}{D_{BH}} + \frac{x_BJ_A - x_AJ_B}{D_{AB}}, \tag{3}$$

$$\rho\frac{dx_H}{d\ell} = \frac{x_HN_A - x_AN_H}{D_{AH}} + \frac{x_HN_B - x_BN_H}{D_{BH}} = \frac{x_HJ_A - x_AJ_H}{D_{AH}} + \frac{x_HJ_B - x_BJ_H}{D_{BH}}. \tag{4}$$

Stoichiometry relations for fluxes and expression for summary flux in our case are

$$N_B = -N_A, \quad N_H = nN_A, \quad N_{tot} = N_A + N_B + N_H = N_H. \tag{5}$$

Below three different approaches, which are based on Eqs. (2)–(4), will be exploited for modeling of external mass transfer for a heterogeneous gas-phase reaction of Eq. (1) type. The field of our interest will be restricted here by forced convection with so-called "low fluxes", i.e. no "high flux" mass transfer correction factors will be considered. As it was pointed out in [7], the case of "low fluxes" is closely approximated in many engineering situations, and most of the published studies of binary forced convection are for this case.

3.1. Simplified general approach of Krishna [6,10]

After taking two independent Maxwell–Stefan equations for diffusion fluxes Eqs. (2) and (4) and making the following formal substitutions:

- concentration gradients $dx_i/d\ell$ are replaced by concentration differences $\Delta x_i = x_{is} - x_{ib}$;
- binary diffusion coefficients D_{ij} are replaced by binary mass transfer coefficients β_{ij};
- the variable value of mole fraction x_i across the diffusion film is replaced by constant referenced value $\tilde{x}_i$ (alternatives for choosing $\tilde{x}_i$ will be discussed below)

one can easily get:

$$\rho\Delta x_A = \frac{\tilde{x}_AJ_H - \tilde{x}_HJ_A}{\beta_{AH}} + \frac{\tilde{x}_AJ_B - \tilde{x}_BJ_A}{\beta_{AB}}, \tag{6}$$

$$\rho\Delta x_H = \frac{\tilde{x}_HJ_A - \tilde{x}_AJ_H}{\beta_{AH}} + \frac{\tilde{x}_HJ_B - \tilde{x}_BJ_H}{\beta_{BH}}. \tag{7}$$

Assuming $\beta_{AH} = \beta_{BH}$ and using the properties of diffusion fluxes and molar fractions:

$$J_B = -(J_A + J_H), \quad \tilde{x}_B = 1 - \tilde{x}_A - \tilde{x}_H,$$

Terms J_B and x_B can be excluded from Eqs. (6) and (7), and the following expressions for diffusion fluxes depending on concentration differences are derived:

$$J_H = -\rho\beta_{AH}\Delta x_H, \tag{8}$$

$$J_A = -\rho\beta_K\left(\Delta x_A + \tilde{x}_A\left(1 - \frac{\beta_{AH}}{\beta_{AB}}\right)\Delta x_H\right). \tag{9}$$

where

$$\beta_K = \left(\frac{\tilde{x}_H}{\beta_{AH}} + \frac{1 - \tilde{x}_H}{\beta_{AB}}\right)^{-1}.$$

The addition of the convective fluxes to Eqs. (8) and (9) yields the following expressions for the total fluxes:

$$N_H = J_H + \tilde{x}_HN_{tot} = -\rho\beta_{AH}\Delta x_H + \tilde{x}_H(N_A + N_B + N_H), \tag{10}$$

$$\begin{aligned} N_A &= J_A + \tilde{x}_AN_{tot} = -\rho\beta_K\left(\Delta x_A + \tilde{x}_A\left(1 - \frac{\beta_{AH}}{\beta_{AB}}\right)\Delta x_H\right) \\ &\quad + \tilde{x}_A(N_A + N_B + N_H). \end{aligned} \tag{11}$$

Strictly speaking, $\tilde{x}_i$ (i = A, H) in Eqs. (9)–(11) should correspond to mixture composition averaged along the film thickness, whereas the limiting values of $\tilde{x}_i$ are x_{ib} (bulk gas, known value) and x_{is} (near surface, unknown value). We assume $\tilde{x}_i = x_{ib}$ (for all approaches considered here and below) following the recommendation [6] that such algorithm simplification is sufficient for the most chemical engineering purposes. Mass transfer coefficients β_{ij} in Eqs. (8)–(11) are defined using traditional empirical correlation for mass transfer from spherical particle [14]:

$$\begin{aligned} Sh_{AH} &= 2 + 0.6Re^{0.5}Sc_{AH}^{0.33}, \quad Sc_{AH} = \frac{\nu}{D_{AH}}, \quad \beta_{AH} = \frac{Sh_{AH}D_{AH}}{d}, \\ Sh_{AB} &= 2 + 0.6Re^{0.5}Sc_{AB}^{0.33}, \quad Sc_{AB} = \frac{\nu}{D_{AB}}, \quad \beta_{AB} = \frac{Sh_{AB}D_{AB}}{d}. \end{aligned} \tag{12}$$

Employing the stoichiometry and the summation relations from Eq. (5), the total fluxes N_A, N_H from Eqs. (10) and (11) are reduced to the following:

if component A is a transport-limiting component ($\Delta x_A = x_{As} - x_{Ab}, \quad x_{As} = 0$):

$$N_A = \frac{\rho \beta_K x_{Ab}}{1 + n x_{Ab}[\beta_K (1 - x_{Hb})((1/\beta_{AB}) - (1/\beta_{AH})) - 1]}, \tag{13}$$

where

$$\beta_K = \left(\frac{x_{Hb}}{\beta_{AH}} + \frac{1 - x_{Hb}}{\beta_{AB}} \right)^{-1},$$

and if H_2 is a transport-limiting component ($\Delta x_H = x_{Hs} - x_{Hb}, \quad x_{Hs} = 0$):

$$N_H = \frac{\rho \beta_{AH} x_{Hb}}{1 - x_{Hb}}. \tag{14}$$

3.2. *General approach based on linearization method, proposed by Stewart, Prober and Toor in [7–9]*

Two independent Maxwell–Stefan equations for diffusion fluxes, Eqs. (2) and (4), can be written in the matrix form:

$$\rho \frac{d\vec{x}}{d\ell} = -[R]\vec{J}; \quad \vec{x} = \begin{pmatrix} x_A \\ x_H \end{pmatrix}; \quad \vec{J} = \begin{pmatrix} J_A \\ J_H \end{pmatrix};$$

$$[R] = \begin{bmatrix} \dfrac{1}{D_0} & \tilde{x}_A \left(\dfrac{1}{D_{AB}} - \dfrac{1}{D_{AH}} \right) \\ 0 & \dfrac{1}{D_{AH}} \end{bmatrix} \tag{15}$$

where

$$D_0 = \left(\frac{\tilde{x}_H}{D_{AH}} + \frac{1 - \tilde{x}_H}{D_{AB}} \right)^{-1}. \tag{16}$$

Two eigenvalues of the inverse matrix $[R]^{-1}$ are D_0 and D_{AH}. Two corresponding eigenvectors $\vec{t}_1$ and $\vec{t}_2$ define the linear substitution of variables

$$\vec{t}_1 = \begin{pmatrix} 1 \\ 0 \end{pmatrix}, \quad \vec{t}_2 = \begin{pmatrix} -\tilde{x}_A \\ 1 - \tilde{x}_H \end{pmatrix}, \tag{17}$$

$$\vec{x} = [T][\vec{x}\,'], \quad \vec{J} = [T][\vec{J}\,'], \quad [T] = \begin{bmatrix} 1 & -\tilde{x}_A \\ 0 & 1 - \tilde{x}_H \end{bmatrix}. \tag{18}$$

Matrix Eq. (15) is transformed to a diagonal form after substitution (17) and (18):

$$\vec{J}\,' = -\rho [D] \frac{d\vec{x}\,'}{d\ell}, \quad [D] = \begin{bmatrix} D_0 & 0 \\ 0 & D_{AH} \end{bmatrix}. \tag{19}$$

After formal application of the empirical binary mass transfer correlations (12) to Eq. (19) the latter ones are transformed as follows:

$$\vec{J}\,' = -\rho [B](\vec{x}\,'_s - \vec{x}\,'_b), \quad [B] = \begin{bmatrix} \beta_0 & 0 \\ \beta_0 & \beta_{AH} \end{bmatrix}, \quad \beta_0 = \frac{D_0 Sh(D_0)}{d},$$

$$\beta_{AH} = \frac{D_{AH} Sh(D_{AH})}{d}. \tag{20}$$

Then we can go back from transformed to ordinary diffusion fluxes in vector form:

$$\vec{J} = [T]^{-1} \vec{J}\,', \quad [T]^{-1} = \begin{bmatrix} 1 & \dfrac{\tilde{x}_A}{1 - \tilde{x}_H} \\ 0 & \dfrac{1}{1 - \tilde{x}_H} \end{bmatrix} \tag{21}$$

or in scalar form

$$J_H = \rho \beta_{AH} (x_{Hb} - x_{Hs}), \tag{21.1}$$

$$J_A = \rho \beta_{AH} \left[\frac{\beta_0}{\beta_{AH}} (x_{Ab} - x_{As}) - \left(1 - \frac{\beta_0}{\beta_{AH}} \right) \frac{\tilde{x}_A}{1 - \tilde{x}_H} (x_{Hb} - x_{Hs}) \right]. \tag{21.2}$$

After adding of convective terms in Eqs. (21.1) and (21.2) the following expressions for total fluxes are got:

$$N_H = \rho \beta_{AH} (x_{Hb} - x_{Hs}) + \tilde{x}_H (N_A + N_B + N_H), \tag{22}$$

$$N_A = \rho \beta_{AH} \left[\frac{\beta_0}{\beta_{AH}} (x_{Ab} - x_{As}) - \left(1 - \frac{\beta_0}{\beta_{AH}} \right) \frac{\tilde{x}_A}{1 - \tilde{x}_H} (x_{Hb} - x_{Hs}) \right] + \tilde{x}_A (N_A + N_B + N_H). \tag{23}$$

We again assume here (as in Section 3.1) that the reference concentrations in Eq. (16), (22) and (23) are taken from the bulk $\tilde{x}_i = x_{ib}$. Then the stoichiometry relations (5) and Eqs. (22) and (23) enable to get direct expressions for total fluxes N_A, N_H:

if A is a transport-limiting component ($x_{As} = 0$)

$$N_A = \frac{\rho \beta_0 x_{Ab}}{1 - n x_{Ab} (\beta_0 / \beta_{AH})}, \tag{24}$$

if H_2 is a transport-limiting component ($x_{Hs} = 0$)

$$N_H = \rho \beta_{AH} \frac{x_{Hb}}{1 - x_{Hb}}. \tag{25}$$

3.3. *Pseudo-binary approach based on film model analytical solution approximation (valid only for reactions $A + nH_2 = B$)*

Earlier attempts to treat the Maxwell–Stefan equations analytically usually led to complex expressions that were too difficult to use [15]. Our aim was to derive an approximate analytical solution for the (de)hydrogenation reaction considering a practically important case $D_{AB} \ll D_{AH} \approx D_{BH}$ in the framework of film model for gas–solid transfer. Here we restrict our consideration to the case of sufficiently large *Sh* numbers (in our experiments $Sh > 10$), and, therefore, an averaged film thickness ($h_D = d/Sh$) is small in comparison with a catalyst pellet diameter *d*. So, planar film may be considered instead of spherical one. Our film model is based on the independent Maxwell–Stefan Eqs. (2) and (4):

$$\rho \frac{dx_A}{d\ell} = \frac{x_A N_H - x_H N_A}{D_{AH}} + \frac{x_A N_B - x_B N_A}{D_{AB}}, \quad 0 \le \ell \le h_d, \tag{26}$$

$$\rho \frac{dx_H}{d\ell} = \frac{x_H N_A - x_A N_H}{D_{AH}} + \frac{x_H N_B - x_B N_H}{D_{BH}}. \tag{27}$$

If the stoichiometry relations, Eq. (5), and $D_{AH} = D_{BH}$ are applied, then Eqs. (26) and (27) are transformed to the dimensionless form

$$\frac{dx_H}{d\xi} = -nf(1 - x_H), \quad 0 \le \xi \le 1, \tag{28}$$

$$\frac{dx_A}{d\xi} = nfx_A - f[1 + F(1 - x_H)], \tag{29}$$

where

$$F = \frac{D_{AH}}{D_{AB}} - 1; \quad f = \frac{N_A h_d}{D_{AH} \rho}; \quad \xi = \frac{\ell}{h_d}; \tag{30}$$

$$\text{at } \xi = 0 \text{ (bulk)}: \; x_H = x_{Hb}; \; x_A = x_{Ab}. \tag{31}$$

The analytical solution of Eq. (28) with the boundary value x_{Hb} (31) is easily got:

$$x_H(\xi) = 1 - (1 - x_{Hb}) \exp(nf\xi), \tag{31.1}$$

then, after substitution of the above expression in Eq. (29), we get:

$$\frac{dx_A}{d\xi} = nfx_A - f[1 + F(1 - x_{Hb})\exp(nf\xi)]. \tag{31.2}$$

The analytical solution of the above equation with the initial value x_{Ab} (31) appears as

$$x_A(\xi) = \{n[x_{Ab} - fF(1 - x_{Hb})\xi] - [1 - \exp(-nf\xi)]\}\frac{\exp(nf\xi)}{n}. \tag{31.3}$$

Now one can readily get the values of molar fractions for both reactants at $\xi = 1$ (near the catalyst surface):

$$x_{Hs} = x_H(1) = 1 - (1 - x_{Hb})\exp(nf), \tag{32}$$

$$x_{As} = x_A(1) = \{n[x_{Ab} - fF(1 - x_{Hb})] - [1 - \exp(-nf)]\}\frac{\exp(nf)}{n}. \tag{33}$$

Here we assume a case of complete external transport control of apparent reaction rate by hydrocarbon A and so $x_{As} = 0$, and Eq. (33) transforms into a transcendent equation with one variable f:

$$n[x_{Ab} - fF(1 - x_{Hb})] = 1 - \exp(-nf). \tag{34}$$

The qualitative consideration of the monotonic behavior of the left part (decreasing) and the right part (increasing) of Eq. (34) with respect to unknown f leads to the conclusion that the unique solution f always exists for arbitrary parameters n, $F > 0$, $0 < x_{Ab} < 1$, $0 < x_{Hb} < 1$. Moreover, the solution f satisfies the following inequality:

$$0 < f < \frac{x_{Ab}}{F(1 - x_{Hb})} = \frac{x_{Ab}}{F(x_{Ab} + x_{Bb})} < \frac{1}{F}.$$

Here we again take into account that for hydrogenation (dehydrogenation) mixtures the condition $D_{AH} \gg D_{AB}$ is valid and, so, according to Eq. (30), $F \gg 1$. At the same time, the absolute value of n is not large for most practically interesting reactions (usually, $|n| \leq 3$, in our case $n = 1$). Thus, the argument of the exponential function in Eq. (34) may be regarded as sufficiently small

$$|n|f < \frac{|n|}{F} \ll 1 \tag{35}$$

and the linear approximation of the exponential term in Eq. (34) is justified

$$\exp(-nf) \approx 1 - nf.$$

After that, the resulting linear equation can be easily solved and the approximate analytic solution of Eq. (34) may be derived

$$f = \frac{x_{Ab}}{1 + F(1 - x_{Hb})}. \tag{36}$$

Substitution of the values f, F from relations (30) into Eq. (36) enables to express the molar flux of A in the conventional form:

$$N_A = \rho\frac{D_0}{h_d}x_{Ab} = \rho\beta_0 x_{Ab}, \tag{37}$$

$$\beta_0 = \frac{D_0 Sh(D_0)}{d}, \quad D_0 = \left(\frac{x_{Hb}}{D_{AH}} + \frac{1 - x_{Hb}}{D_{AB}}\right)^{-1}. \tag{38}$$

The value D_0 (38) is exactly the same as in Eq. (16), and it represents a pseudo-binary analog of the effective diffusion coefficient in the case when A (hydrocarbon) is a transport-limiting reactant. As it will be shown below, the opposite case of a transport-limiting reactant H_2 is only feasible for extremely small hydrogen bulk concentrations and, therefore, D_0 is valid for the whole experimental range of bulk mixture compositions. If nevertheless H_2 is transport limiting, its flux is defined in the same manner as for two previous general approaches (Eq. (14) or (25)).

It is worthy to note, that the considered pseudo-binary approach given by Eqs. (37) and (38) should be used without addition of convective term or any correction factor as well.

The approximation error for the considered pseudo-binary approach can be derived by the estimation of the neglected tail of the exponential series

$$\left|\frac{N_A - N_A^*}{N_A}\right| < \frac{|n|}{2F}, \tag{39}$$

where N_A is the approximate solution, given by Eqs. (37) and (38); N_A^* is the exact solution of film model boundary problem, Eqs. (28)–(31).

Eq. (32) enables to get the asymptotic estimation (for $|n| \leq F$) for variation of hydrogen molar fraction across the film:

$$\frac{x_{Hb} - x_{Hs}}{1 - x_{Hb}} \approx \frac{|n|}{F} \ll 1. \tag{40}$$

From estimation (40) it follows that in case $D_{AB} \ll D_{AH}$ (or $F \gg 1$) this variation is small enough, that is, hydrogen fraction across the film is nearly constant. This conclusion seems very important, because physical properties of the H_2–hydrocarbons mixture strongly depend on the hydrogen fraction. Thus, the use of traditional empirical correlations for gas–solid transfer (which, as a rule, are derived under constant physical properties of fluid) gets the theoretical background.

Furthermore, the developed approach enables to derive the criterion of a so-called *diffusion* stoichiometry, that is, a point where the transport-limiting component (A or H_2 in our case) changes. Diffusion stoichiometry (under complete external transport control of reaction rate) assumes the zero concentrations for both components (AMS and H_2) on the surface. Insertion $x_{As} = 0$, $x_{Hs} = 0$ into Eqs. (32) and (33) and taking into account Eq. (36) (the mathematical details of the derivation are omitted here) gives the approximate conditions for the diffusion stoichiometry:

$$x_{Ab} \approx \frac{(F - 1 - ny_{Ab})y_{Ab}}{F}, \tag{41}$$

$$x_{Hb} \approx \frac{1 + ny_{Ab}}{F},$$

where

$$y_{Ab} = \frac{x_{Ab}}{1 - x_{Hb}} = \frac{x_{Ab}}{x_{Ab} + x_{Bb}} = \text{const.}$$

Finally, it is useful to apply the obtained analytical estimations for our reaction systems.

For AMS hydrogenation ($T = 473$ K, $D_{AB} = 5.0 \times 10^{-6}\ \text{m}^2/\text{s}$, $D_{AH} = 7.5 \times 10^{-5}\ \text{m}^2/\text{s}$): $n = 1$, $F \approx 14$, $n/F \approx 0.071 \ll 1$,

- variation of hydrogen molar fraction across the film does not exceed 7%;
- approximation error (Eq. (39)) is practically negligible $n/(2F) < 4\%$;
- hydrogen bulk mole fraction for diffusion stoichiometry point (Eq. (41) at $y_{Ab} = 1$) is $x_{Hb} \approx 14\%$.

For 1-octene hydrogenation ($T = 473$ K, $D_{AB} = 4.0 \times 10^{-6}\ \text{m}^2/\text{s}$, $D_{AH} = 6.9 \times 10^{-5}\ \text{m}^2/\text{s}$) the estimations are very similar to AMS. So, the use of the suggested pseudo-binary external mass transfer approach for the considered reaction systems is justified.

3.4. Gas-pellet heat transfer coefficient

Heat transfer coefficient α is found from correlation similar to Eq. (12):

$$\alpha = \frac{Nu\lambda}{d}A_F, \quad Nu = 2 + 0.6Re^{0.5}Pr^{0.33}, \tag{42}$$

$$A_F = \frac{\phi}{\exp(\phi) - 1}, \quad \phi = \frac{N_A C_A + N_H C_H + N_B C_B}{\alpha}. \tag{43}$$

The Ackermann correction factor A_F (together with heat transfer rate factor ϕ) reflects the influence of finite mass fluxes on the heat transfer coefficient. Numerical estimations of the values A_F and ϕ have shown that

$$|\phi| < 0.02, \quad |A_F - 1| < 0.01,$$

i.e. the Ackermann correction factor can be neglected in our case $A_F \approx 1$. Heat conductivity of a mixture (H_2 + hydrocarbons) is calculated using the special empirical method from [16]:

$$\lambda = b\lambda_{\max} + (1-b)\lambda_{\min}, \quad b = 0.32(1-x_{Hb}) + 0.8x_{Hb},$$

$$\lambda_{\max} = \lambda_A(1-x_{Hb}) + \lambda_H x_{Hb}, \quad \lambda_{\min} = \left[\frac{x_{Hb}}{\lambda_H} + \frac{(1-x_{Hb})}{\lambda_A}\right]^{-1}.$$

3.5. Calculation of the bulk-surface temperature rise

For all the considered above approaches the bulk-surface temperature rise is calculated as

$$\Delta T = T_s - T_b = \frac{WQ}{\alpha},$$

where reaction rate W is defined by the molar flux of the transport-limiting component:

$$W = N_A \ (\text{if } nN_A < N_H), \quad W = N_H \ (\text{if } nN_A > N_H).$$

Molar fluxes N_A and N_H are calculated from Eqs. (13) and (14), (24), (37) and (38). The point of diffusion stoichiometry is defined by condition $nN_A = N_H$.

In the case of noticeable reversibility of hydrogenation reaction the developed pseudo-binary approach (Section 3.3) enables to apply the straightforward modification, taking reversibility into account unlike two general approaches (Sections 3.1 and 3.2). Under conditions of thermodynamic equilibrium the near surface concentration of A may be nonzero. Then the bulk-surface temperature rise should be calculated as

$$\Delta T = T_s - T_b = \frac{\rho\beta_0(x_{Ab} - x_{As})Q}{\alpha}. \tag{44.1}$$

Thermodynamic equilibrium on the catalyst surface assumes the relation:

$$x_{As}x_{Hs} = \frac{K_R(T_s)}{P}x_{Bs}. \tag{44.2}$$

The pseudo-binary approach justifies negligible H_2 variation across the external film, Eq. (40), and the reaction stoichiometry (Eqs. (1) and (5)) get the equivalence (with the opposite sign) of A and B mole fluxes:

$$x_{Hs} = x_{Hb}, \tag{45.1}$$

$$N_A = \beta\rho(x_{Ab} - x_{As}) = \beta\rho(x_{Bs} - x_{Bb}) = -N_B. \tag{45.2}$$

After insertion of Eq. (45.1) into Eq. (44.2) and reduction of Eq. (45.2) to the form

$$x_{Ab} + x_{Bb} = x_{As} + x_{Bs} = 1 - x_{Hb}, \tag{45.3}$$

the following system of two linear equations with unknown x_{As}, x_{Bs} is obtained

$$x_{As}x_{Hb} = \frac{K_R(T_s)}{P}x_{Bs}, \tag{46.1}$$

$$x_{As} + x_{Bs} = 1 - x_{Hb}. \tag{46.2}$$

The only one solution of the system (46.1) and (46.2) is needed:

$$x_{As} = \frac{K_R(T_s)(1-x_{Hb})}{[Px_{Hb} + K_R(T_s)]}. \tag{47}$$

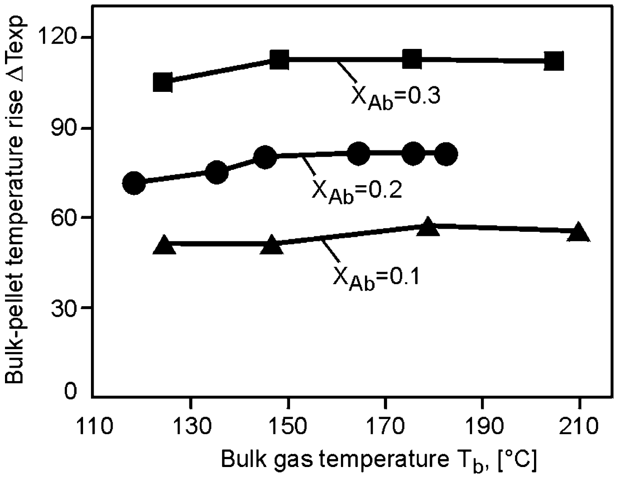

Fig. 1. Impact of a gas flow temperature on the experimentally measured bulk-pellet temperature rise during AMS hydrogenation.

And finally, after substitution of Eq. (47) into Eq. (44.1) the transcendent equation for the unknown temperature T_s and the corresponding ΔT is got:

$$\Delta T = T_s - T_b = \left(\frac{\rho\beta_0 x_{Ab}Q}{\alpha}\right)\left\{1 - \frac{K_R(T_s)(1-x_{Hb})}{x_{Ab}[Px_{Hb} + K_R(T_s)]}\right\}. \tag{48}$$

4. Results

4.1. Experimental evidence for the external transport control of reaction rate

Large gas-pellet experimental temperature rises (100–200 °C) both for AMS and 1-octene hydrogenation, lead to the suggestion that the reaction rate is controlled by the external transport. This is supported by the fact that the temperature rises measured for 3.5% Pd/γAl_2O_3 and 15% Pt/γAl_2O_3 pellets are almost equal (with all other conditions being unchanged). Additional confirmation for the complete control of reaction rate by the external transport has been got by varying the gas bulk temperature within the interval 120–210 °C (Fig. 1) and gas flow rate Re = 30–500 (Fig. 2): the experimental values of the gas-pellet temperature rise remained

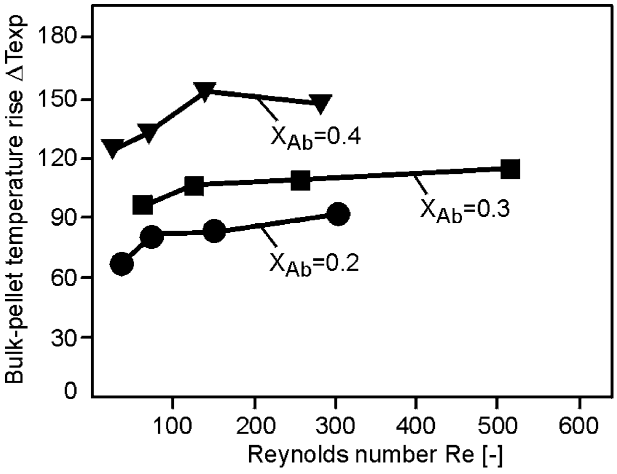

Fig. 2. Impact of Re number on the experimentally measured bulk-pellet temperature rise during AMS hydrogenation.

practically constant under these variations. The slight increase of the experimental curves $\Delta T(Re)$ in Fig. 2 in the region of low Re values may be explained by the increase ratio of thermal/diffusion film thicknesses (assuming empirical correlations from Eqs. (12) and (42)):

$$\Delta T(Re) \sim \frac{\beta(Re)}{\alpha(Re)} \sim \frac{h_h(Re)}{h_d(Re)} \approx \frac{Sh(Re)}{Nu(Re)} = \frac{2+0.6Re^{0.5}Sc^{0.33}}{2+0.6Re^{0.5}Pr^{0.33}}. \qquad (49)$$

Under condition $Sc/Pr = a/D_* = Le > 1$; $h_h = d/Nu$; $h_d = d/Sh$, the right part of Eq. (49) can increase from unity (at $Re = 0$) to the larger values together with increasing Re number. In the region of large Re numbers the ratio of thermal/diffusion film thicknesses becomes independent on Re (where $Sh \gg 2$, $Nu \gg 2$):

$$\frac{h_h}{h_d} \approx \left(\frac{Sc}{Pr}\right)^{0.33} = Le^{0.33}, \qquad (50)$$

together with the gas-pellet temperature rise $\Delta T(Re)$, which approaches its upper limit

$$\Delta T = \frac{Le^{-0.67} Q x_b}{C_b}.$$

4.2. Comparison of the different external mass transfer approaches

Fig. 3(a) and (b) compares the experimental and calculated values of the gas-pellet temperature rise under AMS and 1-octene hydrogenation as a function of hydrocarbon vapor fraction. The usage of conventional (Fick) approach, which is based on the binary diffusion coefficient D_{AH}, results in extremely large values of the temperature rise as compared to the experimental data. In the considered case ($D_{AH}/D_{AB} > 10$) the binary approach is valid only for very small molar hydrocarbon fractions (less than 0.03) and corresponding small temperature rises 10–30 °C. Three other methods based on multicomponent diffusion theory, give close results with the maximum deviation from the experimental data of about 20%. This value seems not bad, if one takes into account that all general methods for diffusion coefficients calculation usually have the same confidence interval [16]. Only for the highest value of AMS and 1-octene molar fraction $x_{Ab} = 0.6$ a marked difference between the experimental points and theoretical curves is observed. The following additional experiments and calculations have been done in order to clarify this effect.

4.3. The possible impact of side and reverse reactions: AMS + H_2

In the course of additional experiments with AMS (Fig. 4(a)) it was found that the values of temperature rise shown in Fig. 3(a) can be reached only if a fresh or regenerated catalyst pellet was used. The measured temperature rise slowly faded (symbols in Fig. 4(a)). The lower values were not dependent on the bulk temperature and Re number as well as the initial higher ones. So the influence of the kinetic factors may be ruled out. The most likely explanation is AMS self-olygomerization that blocked essential (but limited) part of the catalyst pellet external surface. Meanwhile the remaining active part of the pellet surface continued to operate under external transfer control. This process of blocking evidently has no influence on the gas–solid heat transfer and, thus, the temperature rise decreases owing to decreasing heat source.

Calculations (by pseudo-binary method) that take into account reversibility of AMS hydrogenation reaction show, that thermodynamic equilibrium is unable to explain the divergence of the upper right experimental point in Fig. 4(a). Meanwhile, accounting for reaction reversibility decreases the theoretical temperature rise in the high temperature region (near the point of diffusion stoichiometry S_D). Diffusion stoichiometry condition for both variants corresponds to high excess of vapor $x_{Ab} \approx 0.85$–0.90 which is in good accordance with theory, Eq. (41). So, hydrogen may theoretically become the limiting transport component only for its very small bulk concentration $x_{Hb} \approx 0.10$–0.15, which was not reached in our experiments. The point of ordinary stoichiometry S_0 ($x_{Ab} = 0.5$) is placed far left from diffusion stoichiometry point. Therefore, the region ($x_{Ab} > 0.65$) is theoretically predicted and experimentally confirmed (the last symbol on the right in Fig. 4(a)), where the gas-surface temperature rise exceeds its adiabatic value.

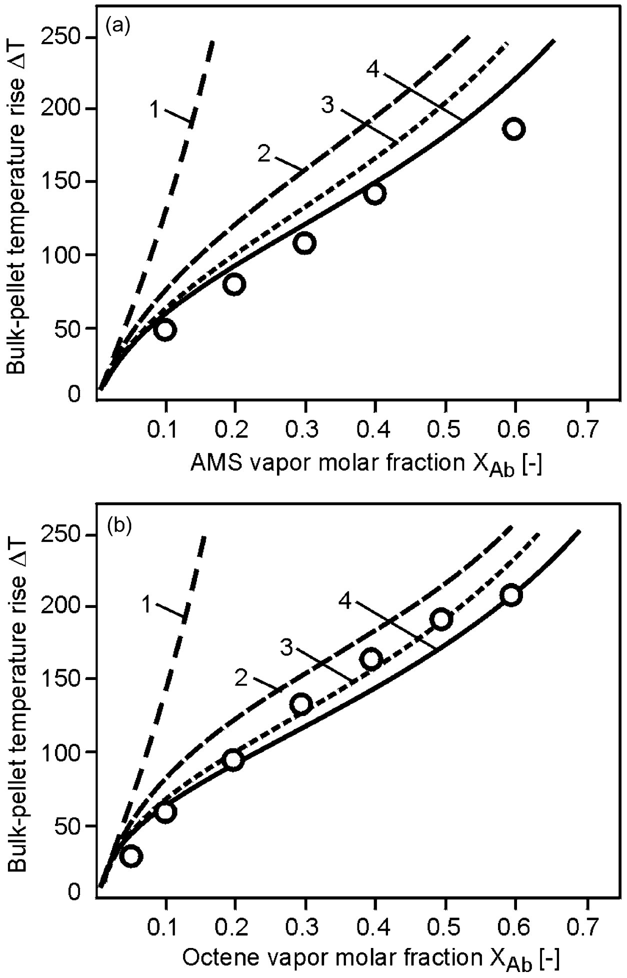

Fig. 3. Comparison of the experimentally measured bulk-pellet temperature rise (symbols) during AMS (a) and 1-octene (b) hydrogenation with the results of calculation by different external mass transfer approaches: (1) binary (Fick) approach with D_{AH}; (2) simplified general multicomponent approach [6,9], Eq. (13); (3) general multicomponent approach, based on linearization [7,8], Eq. (24); (4) pseudo-binary approach for reactions $A + nH_2 = B$ (this work), Eqs. (37) and (38).

4.4. Diluted mixture: AMS + cumene + H_2

A few experiments were made with a mixture of AMS and cumene vapors (AMS:cumene = 1:2). The expected decrease of the gas-pellet temperature rise in Fig. 4(b) (in comparison with undiluted AMS in Fig. 4(a)) is accompanied by the same type of divergence between the experimental data and the theoretical curve. This divergence occurs for sufficiently high bulk vapor fraction ($x_{Ab} + x_{Bb}$) > 0.5. Reaction reversibility does not play significant role in this case because the pellet temperature is lower then that of undiluted AMS. Therefore, the impact of possible side reaction (AMS olygomerization) remains the most appropriate explanation for the observed discrepancy.

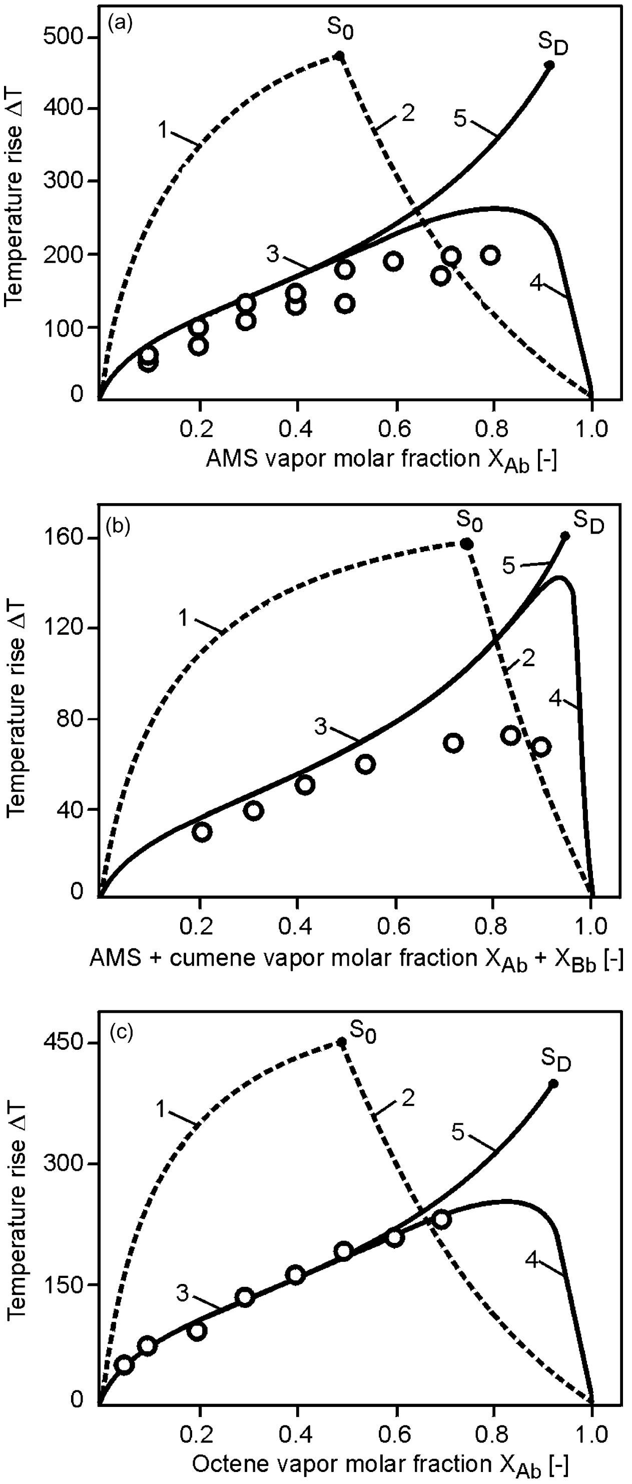

Fig. 4. Comparison of the experimentally measured bulk-pellet temperature rise (symbols) with the calculations during hydrogenation: (a) AMS, (b) mixture (33% AMS + 67% cumene), (c) 1-octene. Adiabatic temperature rise (dashed line): (1) hydrocarbon-limiting branch, (2) hydrogen-limiting branch; S_0: point of ordinary stoichiometry. Results of calculation by the pseudo-binary approach: (3) hydrocarbon external transfer-limiting branch, (4) hydrogen external transfer-limiting branch, (5) reverse reaction is neglected; S_D: point of diffusion stoichiometry.

4.5. *Bulk gas composition: octene + H_2*

Comparison of the experimental and calculated data for 1-octene hydrogenation in Fig. 4(c) reveals better correspondence than that of AMS. The incompatibility between the theoretical curve and the experimental point at $x_{Ab} = 0.6$ in Fig. 3(b) vanishes in Fig. 4(c), when we take into account the reaction reversibility. The point of diffusion stoichiometry and the values of theoretical temperature rise for 1-octene are practically identical to respective values in the AMS case. Excellent correspondence of the experiment and theory for 1-octene may be provided by the absence of noticeable side reactions.

4.6. *Analysis of external mass transfer (AMS hydrogenation in a fixed-bed reactor)*

The experimental data on vaporized AMS hydrogenation in a fixed-bed reactor (2–3 mm spherical catalytic pellets 3.5% Pd/γ-Al_2O_3) is analyzed by means of analytical solution of simple mathematical model of a plug-flow reactor. Nevertheless, change of reacting mixture volume is found essential and is taken into account. The basic assumption is that hydrogenation occurs under control of AMS vapor external mass transfer. The pseudo-binary diffusion coefficient (Eq. (38)) is used.

A plug-flow reactor model includes two material balance equations for AMS vapor and mixture:

$$\frac{d}{dz}(Nx_A) = N\frac{dx_A}{dz} + x_A\frac{dN}{dz} = -r, \quad 0 \le z \le L, \tag{51}$$

$$\frac{dN}{dz} = -r, \tag{52}$$

$$x_A(0) = x_A^{in}; \quad N(0) = N^{in}.$$

After insertion of Eq. (52) in Eq. (51) and introducing dimensionless axial coordinate $z' = z/L$ we get

$$\frac{dx_A}{dz'} = -\frac{rL}{N}(1 - x_A), \quad 0 \le z' \le L, \tag{53}$$

$$x_A(0) = x_A^{in}.$$

The apparent reaction rate under complete external transfer control is first order on AMS vapor

$$r = \beta S \rho x_A. \tag{54}$$

Then, Eq. (53) is reformed via Eq. (54) to the following non-linear problem

$$\frac{dx_A}{dz'} = -kx_A(1 - x_A), \quad 0 \le z' \le L, \tag{55}$$

$$x_A(0) = x_A^{in},$$

where

$$k = \frac{\beta S \rho L}{N} = \frac{\beta S L}{u}. \tag{56}$$

Generally speaking, coefficient k in Eq. (56) undergoes variation along the reactor length (owing to variation of β and u). Nevertheless, estimations made under experimental conditions have shown that this variation does not exceed 3–5%:

$$k \approx \text{const}.$$

After that, the analytical solution of Eqs. (5) and (6) can be derived:

$$x_A^{out} = \frac{A\,\exp(-k)}{1 + A\,\exp(-k)}, \tag{57}$$

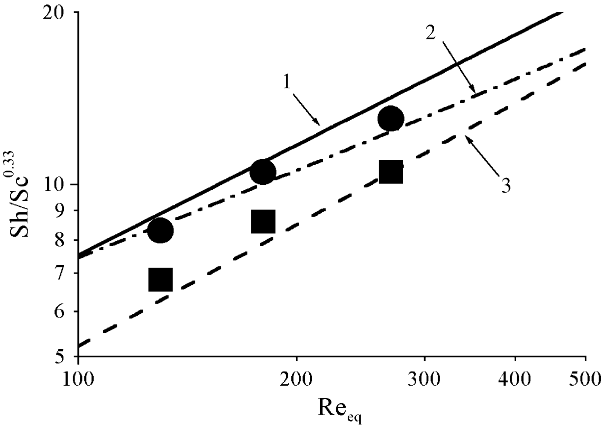

Fig. 5. Comparison of the experimental data on AMS hydrogenation under external mass transfer control in a fixed-bed reactor (circles—$L = 12$ mm; squares—$L = 20$ mm) with gas–solid transport correlations from Ref. [17]: (1) Aerov and Todes, Eq. (61); (2) McCounachie and Thodos, Eq. (62); (3) Bradshaw and Bennet, Eq. (63). The experimental data is transformed into logarithmic coordinates (Re_{eq}–$Sh/Sc^{0.33}$) by means of the pseudo-binary diffusion coefficient Eq. (38).

where

$$A = \frac{x_A^{in}}{1 - x_A^{in}}.$$

Eq. (57) may be inverted so as to express k through inlet and outlet fractions of AMS vapor:

$$k = \ln\left(\frac{x_A^{in}(1 - x_A^{out})}{x_A^{out}(1 - x_A^{in})}\right). \tag{58}$$

Therefore, the algorithm of transforming the values of AMS experimental conversion X_{AMS} to Sh number is the following:

1. Mole fractions of AMS vapor at the outlet are restored:

$$x_A^{out} = \frac{1 - X_{AMS}}{(1/x_A^{in}) - X_{AMS}}. \tag{59}$$

2. The value of k is calculated via Eq. (58).
3. Mass transfer coefficient β is calculated by Eq. (56) from known k.
4. The pseudo-binary diffusion coefficient is calculated through Eq. (38) with $x_{Hb} = x_H^{in}$.
5. Experimentally based Sh and Sc numbers are calculated

$$Sh = \frac{\beta d_{eq}}{D_0}, \quad Sc = \frac{\nu}{D_0}. \tag{60}$$

After all, the experimental data was plotted in logarithmic coordinates ($Sh/Sc^{0.33}$–Re) in Fig. 5. The following three empirical gas–solid mass transport correlations for a fixed bed of spherical particles from literature [17] were also plotted in Fig. 5 and compared with the experimental data:

- M.E. Aerov and O.M. Todes:

$$Sh/Sc^{0.33} = 0.395 Re_{eq}^{0.64}, \tag{61}$$

- I.T. McCounachie and G. Thodos:

$$Sh/Sc^{0.33} = \frac{0.468 Re_{eq}}{1.18 Re_{eq}^{0.41} - 1.52}, \tag{62}$$

- R.D. Bradshaw and C.O. Bennet:

$$Sh/Sc^{0.33} = 0.201 Re_{eq}^{0.707}. \tag{63}$$

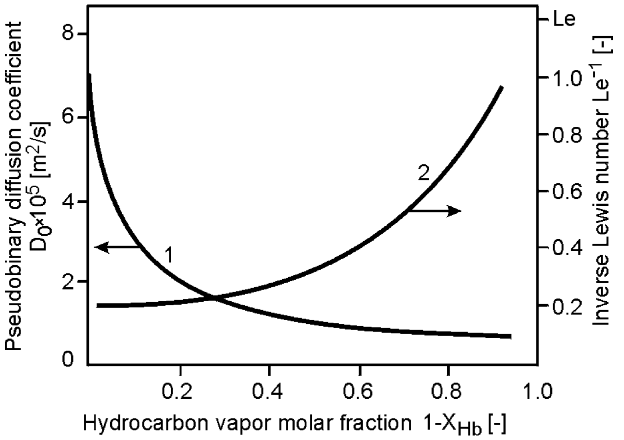

Fig. 6. The impact of hydrocarbon mole fraction on the pseudo-binary diffusion coefficient and the inverse Lewis number (AMS hydrogenation data at $T = 473$ K).

The correlations (61)–(63) are based on the equivalent values of Re and interstitial channel diameter:

$$Re_{eq} = \frac{G d_{eq}}{\varepsilon \mu}, \quad d_{eq} = \frac{4\varepsilon}{S}, \quad S = \frac{6(1 - \varepsilon)}{d}. \tag{64}$$

The agreement between all three correlations and the experimental data may be considered as good, especially if one takes into account that a confidence interval for such empirical correlations usually expands over 15% up and down.

The noticeable shift down for the experimental data with the larger height of catalyst bed (20 mm instead of 12 mm) may be explained in the following way. The increased AMS conversion under near adiabatic conditions (67–71% instead of 52–60% for shorter bed) results in the increased catalyst temperature at the outlet which leads to the increased impact of side reaction (AMS olygomerization) considered earlier in Section 4.3. In any way, the experimental $Sh/Sc^{0.33}$ dependence on Re number with power 0.6–0.7 definitely indicates on complete external mass transfer control of AMS hydrogenation rate, and the pseudo-binary approach successfully predicts the observed tendency.

5. Discussion

5.1. The physical sense of the pseudo-binary approach for reactions of hydrogenation (or dehydrogenation) $A + nH_2 = B$

Contrary to the independent (Fick) diffusion treatment, under the pseudo-binary approach the value of effective diffusion coefficient and the Lewis number are both strongly bulk composition-dependent (Fig. 6). The inverse Lewis number is significantly smaller than unity. Therefore the adiabatic temperature rise ΔT_{ad} exceeds the bulk-pellet temperature rise ΔT (under the external transport control) in the left parts of Fig. 4(a)–(c) in accordance with the equations:

$$\Delta T = \frac{Le^{-0.67} Q x_b}{C_b} = Le^{-0.67} \Delta T_{ad}, \tag{65}$$

$$Le = \frac{\lambda}{C_b \rho D}, \quad \Delta T_{ad} = \frac{Q x_b}{C_b}. \tag{66}$$

From a formal point of view, the pseudo-binary approach is equivalent to consideration of hydrogen as inert component in reacting mixture (because of its comparatively high diffusivity). The physical properties of hydrocarbon reactant A are usually similar to hydrocarbon product B. Therefore, multicomponent diffusion of components A and B in ternary mixture with hydrogen is well approximated by pseudo-binary diffusion of A and B with the effective coefficient D_0 (Eq. (38)), this coefficient depends on the hydrogen fraction. As a relative variation of hydrogen fraction across the film is small, this coefficient remains nearly constant across the film. Another important feature of the coefficient D_0 is that it reflects intrinsic physical property of mixture, if condition $D_{AH} = D_{BH} \gg D_{AB}$ takes place. Actually, in this case light molecules of hydrogen do not influence directly the mutual diffusion of heavy molecules A and B. The variation of hydrogen partial pressure influences exclusively on the vapor partial pressure of hydrocarbons and by this way changes implicitly the value of the diffusion coefficient:

$$\frac{x_H}{D_{AH}} \ll \frac{1-x_H}{D_{AB}}, \quad D_0 \approx \frac{D_{AB}}{1-x_H} = D_{AB}\left(\frac{P}{P-P_H}\right). \tag{67}$$

5.2. Generalization of the pseudo-binary approach on a case of several reactions or inert components

Formal consideration of hydrogen as inert enables to get expression for effective diffusion coefficient D_0 more easily and directly from Maxwell–Stefan Eqs. (2)–(4), if we take into account that $N_B = -N_A$, $n = 0$, $N_H = 0$. Using this idea, one may generalize the pseudo-binary approach on a case of several simultaneous reactions of hydrogenation (or dehydrogenation) in a complex mixture of hydrocarbons:

$$A_i + n_iH_2 = B_i, \quad i = 1, 2, \ldots, M.$$

Maxwell–Stefan equations for $(2M+1)$-component mixture [4,5] are taken as a starting point:

$$\rho\frac{dx_i}{d\ell} = \sum_{j \neq i}\frac{N_jx_i - N_ix_j}{D_{ij}}. \tag{68}$$

Inert but sufficiently heavy components C_k ($k = 1, 2, \ldots, K$) are also admitted to be present in the mixture. If physical properties of each pair (A_i, B_i) are close and all hydrocarbon molecules are sufficiently heavy in comparison with hydrogen, then the following conditions are valid:

$$\begin{aligned} &D_{A_iH} \approx D_{B_iH} \gg D_{A_iB_i}, \quad D_{A_iH} \approx D_{B_iH} \gg D_{A_iC_k}, \quad k = 1, 2, \ldots, K; \\ &D_{A_iA_j} \approx D_{B_iA_j} \approx D_{A_iB_j} \approx D_{B_iB_j}, \quad i = 1, 2, \ldots, M, \quad j = 1, 2, \ldots, M, \quad i \neq j. \end{aligned} \tag{69}$$

Substitution $n_i = 0$, $N_H = 0$, $N_{A_i} = -N_{B_i}$ into the Maxwell–Stefan Eq. (68) and taking into account Eq. (69) leads to the following expression for the effective diffusion coefficient D_{0_i} (for transport-limiting component A_i):

$$\frac{1}{D_{0_i}} = \frac{x_{Hb}}{D_{A_iH}} + \frac{x_{A_ib} + x_{B_ib}}{D_{A_iB_i}} + \sum_{j=1, j \neq i}^{M}\frac{x_{A_jb} + x_{B_jb}}{D_{A_iA_j}} + \sum_{k=1}^{K}\frac{x_{C_k}}{D_{A_iC_k}}. \tag{70}$$

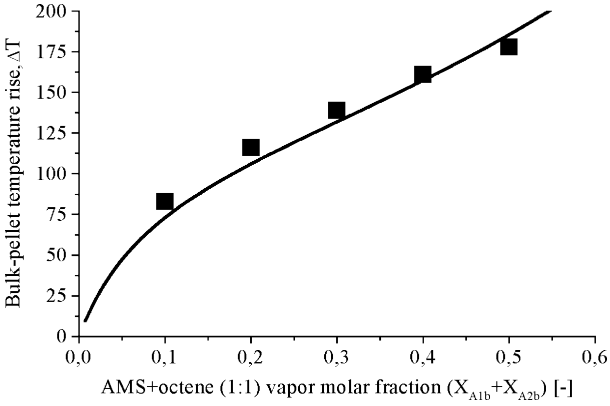

Fig. 7. Comparison of the experimentally measured bulk-pellet temperature rise (symbols) during AMS + 1-octene equimolar (1:1) mixture hydrogenation with the results of calculation by the pseudo-binary approach, generalized for several reactions $A_i + n_iH_2 = B_i$, $i = 1, 2, \ldots$, with the effective diffusion coefficients for AMS and 1-octene D_{0_1}, D_{0_2} given by Eq. (70).

In order to verify the generalized Eq. (70), the additional experimental data from [1] was used, i.e. the bulk-pellet temperature rise measurements in a single-pellet reactor during hydrogenation of AMS with 1-octene equimolar mixture of vapors. Calculations were again based on the assumption that both simultaneous reactions are controlled by the external mass transfer of AMS and 1-octene vapors. The corresponding diffusion coefficients D_{0_1}, D_{0_2} were calculated by the pseudo-binary approach with Eq. (70). The result of comparison is given in Fig. 7 and seems good. Of course, the additional experimental verification with different mixtures would be useful in future.

6. Conclusions

Several gas–solid interfacial mass transfer theoretical approaches were employed to analyze the experimental data on catalytic hydrogenation α-methylstyrene and 1-octene under external transfer control. The binary diffusion (Fick) approach fails to describe the obtained data even in a qualitative sense. Two general approaches to multicomponent mass transfer and the developed pseudo-binary method were successfully applied to analyze these experiments. All three methods give rather close results, with maximum deviation from experimental data and from each other less than 20%.

For hydrogenation (or dehydrogenation) of vaporized hydrocarbons the pseudo-binary approach is recommended. It does not require cumbersome matrix operations in comparison with general multicomponent methods and does not require any correction factors. This advantage may become especially significant for complex mixtures of hydrocarbons and/or several reactions. The developed here pseudo-binary approach is grounded on the approximate analytical solution of the film model. The obtained solution enables to get the rigorous conditions of applicability for our pseudo-binary approach to reactions $A + nH_2 = B$, to estimate hydrogen variation across the film, to find out the point of diffusion stoichiometry, to take into account the reaction reversibility in a simple way. All these details could hardly be accessible by means of general multicomponent approaches.

The resulting pseudo-binary diffusion coefficient (unlike usual pseudo-binary treatment) does not depend on stoichiometric coefficients and has clear physical meaning. Thus the usage of traditional empirical correlations for interphase transfer (which are derived from independent diffusion or heat exchange experimental data) gets the solid theoretical background. Also the convenience of usage of a variety of traditional criteria, which incorporate into itself diffusion coefficient, may play not the last role in preferring the pseudo-binary approach for hydrogenation (dehydrogenation) of vaporized hydrocarbons under external transfer control.

References

[1] V.A. Kirillov, A.V. Kulikov, N.A. Kuzin, A.B. Shigarov, Experimental study of heat regimes on a dry, partially or completely wetted catalyst particle, Chem. Eng. J. 98 (2004) 219–235.

[2] M.R. Khadilkar, P.L. Mills, M.P. Dudukovic, Trickle-bed reactor models for systems with a volatile liquid phase, Chem. Eng. Sci. 54 (1999) 2421–2431.

[3] A.B. Shigarov, A.V. Kulikov, N.A. Kuzin, V.A. Kirillov, Modeling of critical phenomena for liquid/vapor–gas exothermic reaction on a single catalyst pellet, Chem. Eng. J. 91 (2003) 205–213.

[4] D.A. Frank-Kamenetskii, Diffusion and Heat Exchange in Chemical Kinetics, Princeton University Press, New Jersey, 1955.

[5] R. Taylor, R. Krishna, Multicomponent Mass Transfer, John Wiley and Sons, NY, 1993.

[6] R. Krishna, J.A. Wesselingh, The Maxwell–Stefan approach to mass transfer, Chem. Eng. Sci. 52 (1997) 861–911.
[7] W.E. Stewart, R. Prober, Matrix calculation of multicomponent mass transfer in isothermal systems, Ind. Eng. Chem. Fundam. 3 (1964) 224–235.
[8] H.L. Toor, Solution of the linearized equations of multicomponent mass transfer. I, AIChE J. 10 (4) (1964) 448–455.
[9] H.L. Toor, Solution of the linearized equations of multicomponent mass transfer. II. Matrix methods, AIChE J. 10 (4) (1964) 460–465.
[10] R. Krishna, A simplified film model description of multicomponent interphase mass transfer, Chem. Eng. Commun. 3 (1979) 29–37.
[11] E.G. Eddings, H.Y. Sohn, Simplified treatment of the rates of gas–solid reactions involving multicomponent diffusion, Ind. Eng. Chem. Res. 32 (1993) 42–51.
[12] V. Alopaeus, On approximate calculation of multicomponent mass transfer fluxes, Comput. Chem. Eng. 26 (2002) 461–466.
[13] A.B. Shigarov, S.I. Fadeev, I.A. Mikhailova, A.V. Kulikov, V.K. Korolev, N.A. Kuzin, V.A. Kirillov, Simplified treatment of mass transfer for gas-phase hydrogenation/dehydrogenation of heavy compounds, Korean J. Chem. Eng. 19 (2002) 252–260.
[14] G.A. Hugmark, Mass and heat transfer from rigid spheres, AIChE J. 13 (1967) 1219–1221.
[15] H. Hsu, R.B. Bird, Multicomponent diffusion problems, AIChE J. 6 (1960) 516–524.
[16] R.C. Reid, J.M. Prausnitz, Properties of Gases and Liquids, McGraw-Hill Book Co., NY, 1977.
[17] M.E. Aerov, O.M. Todes, Hydraulic and Thermal Fundamentals of a Fixed Bed and Fluidized Bed Reactor Operation, Khimia, Leningrad Department (in Russian), 1968.